Performance Analysis of Photovoltaic-Thermal Liquid Collector by CFD Simulation

Harsh Manani

Department of Mechanical Engineering

Indian Institute of Technology Bombay

Abstract

Aim of this case study is to calculate thermal and electrical efficiency of solar photovoltaic-thermal collector with water used as a fluid. Efficiency of solar PV system decreases as temperature of silicon cell increases. In solar PVT system, water is used as a fluid to decrease temperature of the silicon cell and increase efficiency of electricity generation. Hot water can be used for heating application. In this case study, steady-state and transient of solar PVT system is done for different mass flow rate of water and different solar radiation using chtMultiRegionFoam.

1. Introduction

Due to growing energy demands and limited fossil fuel resources, use of solar photovoltaic is increasing every year. Efficiency of solar PV depends on temperature of silicon cell. In solar PVT system, water is used to reduce the temperature of silicon cell and water can be used for heating applications. This system gives combined output of solar PV and solar thermal collector.

2. Problem Statement

In this problem, a section of solar PVT system containing one water pipe is considered. Geometry and dimensions are given in figure 1. Mass flow rate of water is taken from 0 to 0.016 kg/s. Two values of solar radiation (700 W/m^2 and 1000 W/m^2) are considered. Value of

heat transfer coefficient is taken as $h = 5.7 + 3.8v$ for glass surface and $h = 2.8 + 3.8v$ for all other surfaces. Length of this geometry is 1.6 m.

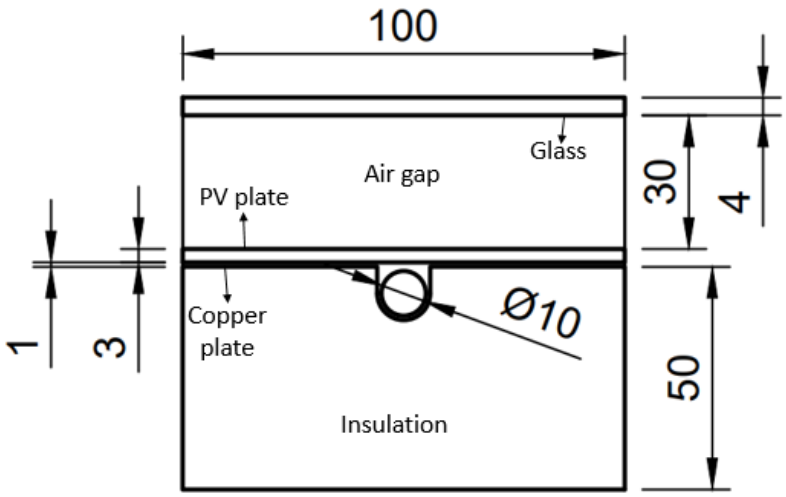

Figure 1: Computational domain

Thermophysical properties of different materials is given in the table.

Component	Specific heat (J/kg K)	Density (kg/m^3)	Thickness (mm)	Thermal conductivity (W/m K)
Glass	820	2515	4	0.98
Air	1007	1.1	30	0.0266
PET	1350	0.14	0.25	0.4
Silicon cell	760	2330	0.3	130
TPT (Tedlar)	1250	1200	2.5497	0.15
Copper plate	385	8933	1	401
Polystyrene insulation	1300	15	50	0.032

Table 1: Thermophysical properties

3. Governing Equations

Continuity Equation

Continuity equation for incompressible fluid is defined as:

$$\frac{\partial u_i}{\partial x_i} = 0 \tag{1}$$

Momentum Equation

Momentum equation for incompressible fluid is defined as:

$$\frac{\partial(\rho u_i)}{\partial t} + \frac{\partial(\rho u_i u_j)}{\partial x_j} = -\frac{\partial p}{\partial x_i} + \mu \frac{\partial^2 u_i}{\partial x_j \partial x_j} + \rho g_i \tag{2}$$

Where u is velocity, ρ is density of the fluid, p is pressure and g_i is gravity, μ is viscosity.

Energy Conservation in Fluid

$$\frac{D}{Dt}\left(\rho\left(e + \frac{1}{2}u_i^2\right)\right) = -\frac{\partial q_i}{\partial x_i} + \frac{\partial^2 \tau_{ij} u_i}{\partial x_j} + \rho g_i u_i + S \tag{3}$$

Where e is internal energy, τ_{ij} is viscous stress, q_i is heat transferred by diffusion, S is heat source term.

Energy Conservation in Solid

$$\frac{\partial(\rho e)}{\partial t} = \frac{\partial}{\partial x_j}\left(\alpha \frac{\partial e}{\partial x_j}\right) \tag{4}$$

Where e is internal energy and α is thermal diffusivity.

Coupling Between Fluid and Solid

Temperature of both fluid and solid is same at the interface.

$$T_f = T_s \tag{5}$$

Heat flux is same for both fluid and solid at the interface.

$$Q_f = -Q_s \tag{6}$$

$$k_f \frac{dT_f}{dn} = -k_s \frac{dT_s}{dn} \tag{7}$$

Where n is normal direction to the wall, k_f and k_s are thermal conductivity of fluid and solid.

4. Simulation Procedure

4.1 Geometry and Mesh

Mesh was created using blockMesh utility in OpenFOAM. Structured mesh is used for this problem. Figure 2 shows mesh for the computational domain which is extended to the third dimension. Mesh is refined near the water pipe to increase accuracy of results. Different cell sets are defined in blockMeshDict for different regions. These cell sets are split into different regions using splitMeshRegions.

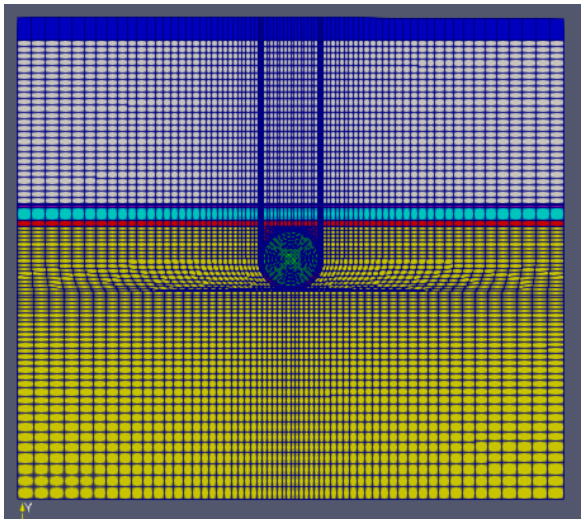

Figure 2: Computational domain with mesh

Grid Independence Study

Grid independence study is done to find minimum number of cells for which results of the simulation does not depend on mesh size. For structured meshes with 63600, 208200, 468480, 880800 cells were considered four grid independence study. Average water outlet temperature for these four meshes is given in figure 3. Temperature change is not significant between mesh 3 and mesh 4. So other simulations were done on mesh 3.

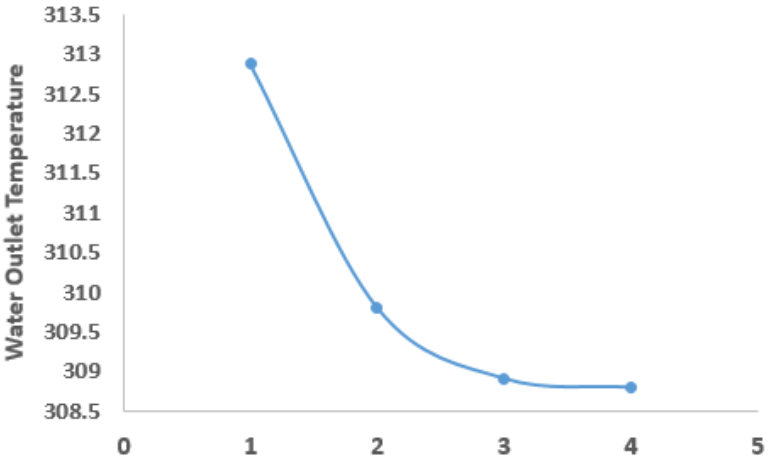

Figure 3: Grid independence study

4.2 Initial and Boundary Conditions (Times New Roman 14pt)

Boundary conditions for fluid:

Boundary	P_rgh	U	T
Inlet	fixedFluxPressure	fixedValue – uniform 0.025	fixedValue – uniform 300
Outlet	fixedValue – uniform 0	pressureInletOutletVelocity	inletOutlet
Wall	fixedFluxPressure	noSlip	compressible::turbulent TemperatureCoupledBaffle Mixed

Table 2: Boundary conditions for fluid

Boundary condition for solid:

Boundary	T
Side walls	zeroGradient
Front and back wall	externalWallHeatFluxTemperature
Top wall	externalWallHeatFluxTemperature
Bottom wall	externalWallHeatFluxTemperature

Table 3: Boundary conditions for solid

For all interfaces between two materials, compressible::turbulentTemperatureCoupledBaffle Mixed boundary condition is used. At t = 0, velocity is uniform 0, pressure is uniform 0 and temperature is uniform 300.

4.3 Solver

chtMultiRegionFoam is used for this problem due to heat transfer between multiple regions. It is a transient solver for fluid flow and solid heat conduction with conjugate heat transfer between solid and fluid regions with buoyancy effect, turbulence, reaction and radiation modelling.

4.4 Post-processing

Average water outlet temperature is calculated by following formula:

$$T_m = \frac{2}{V_m R^2} \int_0^R T(r) V(r) r dr \tag{8}$$

Thermal efficiency of the PVT system can be calculated by following formula:

$$\eta_{th} = \frac{\dot{m} C_p (T_o - T_i)}{A \times G} \tag{9}$$

Where η_{th} is thermal efficiency, m is mass flow rate, C_p is heat capacity of water, T_o and T_i are water outlet and inlet temperature, A is area of the collector, G is solar irradiance.

Electrical efficiency of the silicon cell is determined from temperature of the silicon cell using following graph.

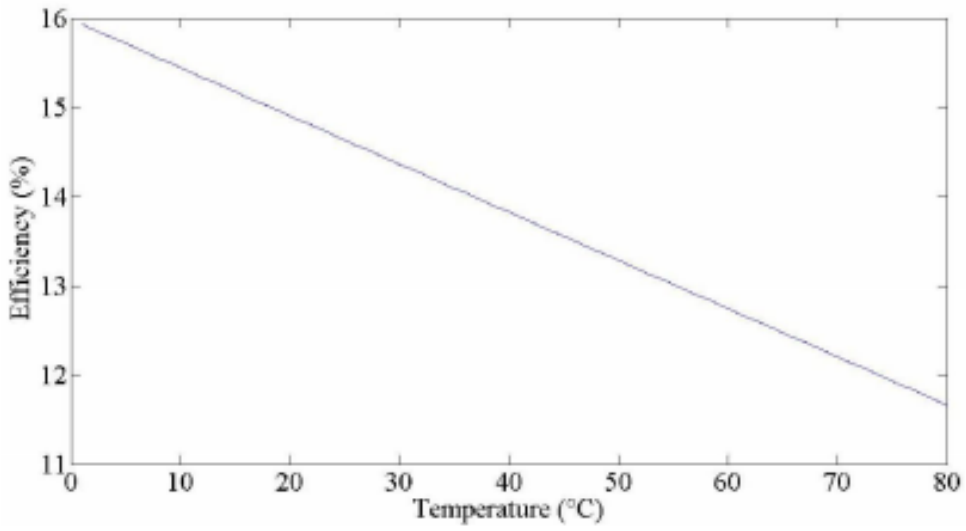

Figure 4: Variation of solar cell efficiency with temperature

5. Results and Discussions

Figure 5 shows variation of water outlet temperature with mass flow rate for solar radiation of 700 W/m^2 and 1000 W/m^2. Figure 6 shows variation of thermal efficiency for 1000 W/m^2 and validation of thermal efficiency. OpenFOAM simulation gives thermal efficiencies very close to the values calculated by Chow T. Figure 7 shows variation of thermal efficiency for 700 W/m^2. Thermal efficiency remains same for both 700 W/m^2 and 1000 W/m^2. Figure 8 shows variation of electrical efficiency for 700 W/m^2 and 1000 W/m^2. Electrical efficiency is higher for 700 W/m^2 due to less amount of heating and lower temperature of silicon cell.

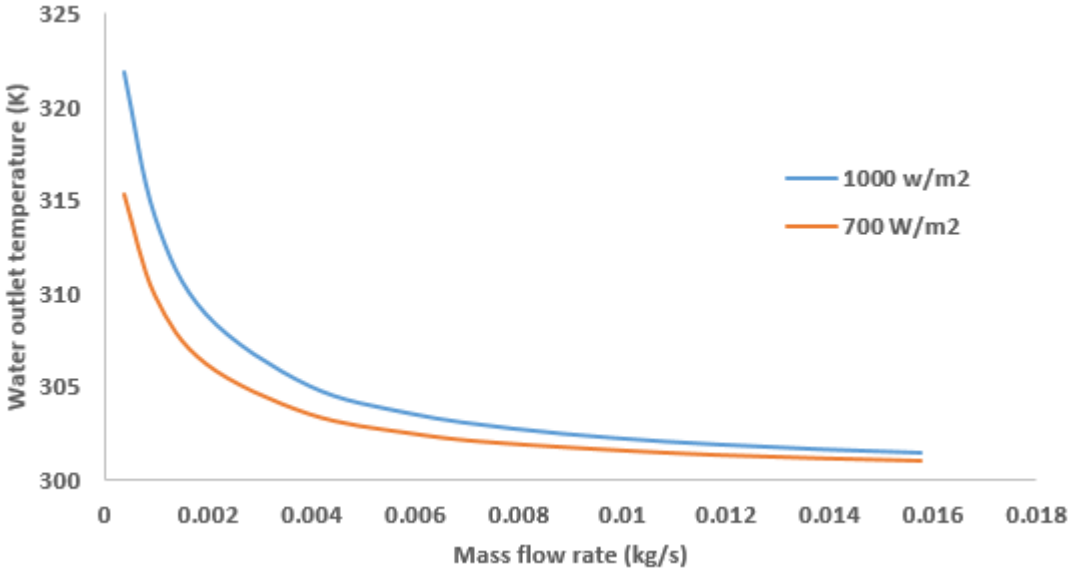

Figure 5: Water outlet temperature

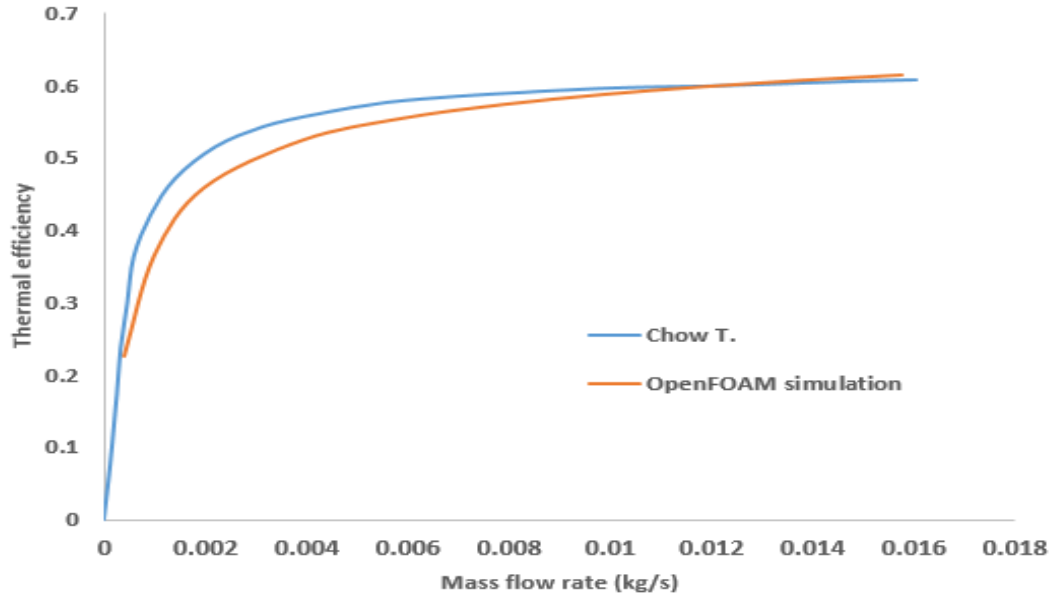

Figure 6: Thermal efficiency for 1000 W/m^2

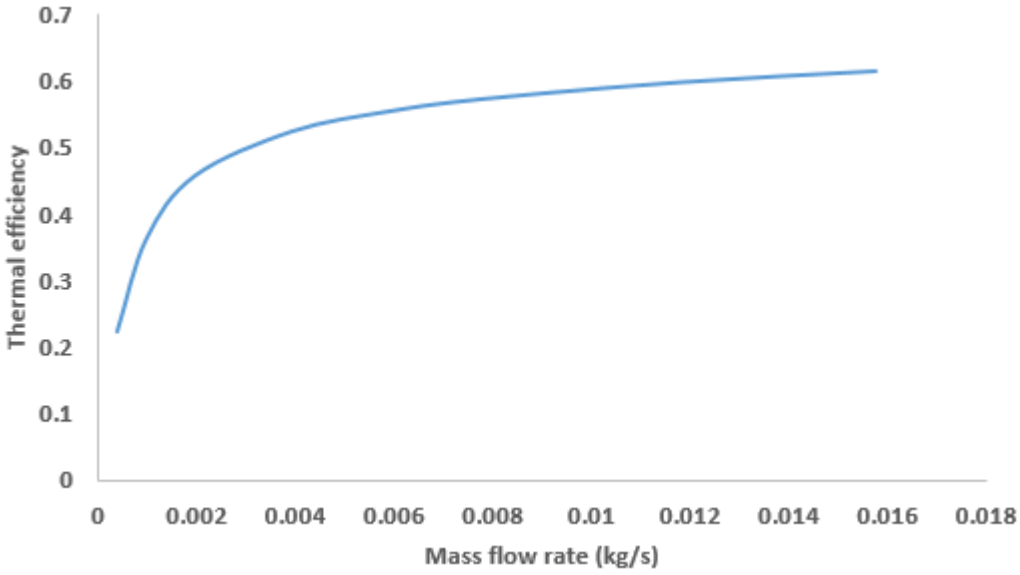

Figure 7: Thermal efficiency for 700 W/m^2

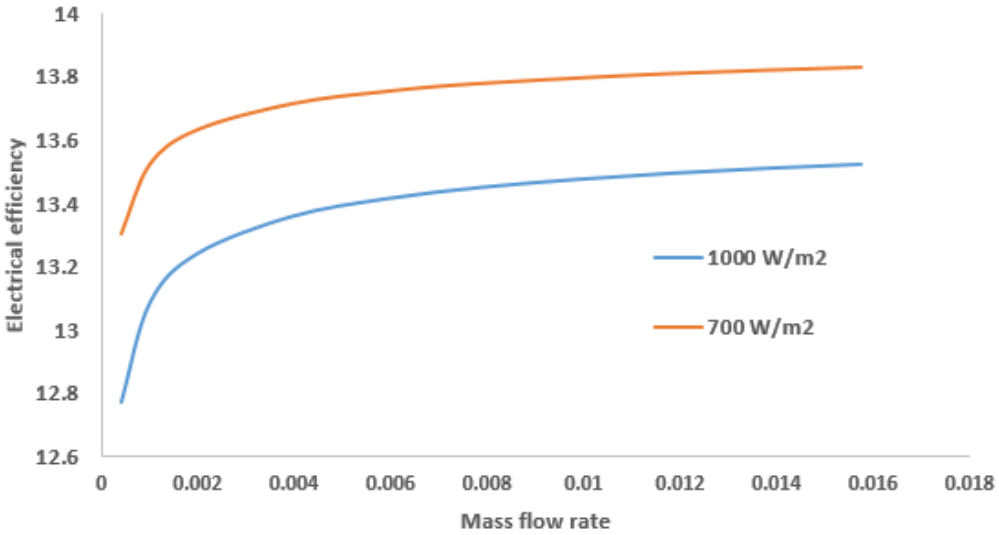

Figure 8: Thermal efficiency for 700 W/m^2 and 1000 W/m^2

Thermal and electrical efficiency increases as mass flow rate of water increases. But water outlet temperature is very low for higher mass flow rate. If we need water for heating applications, then lower mass flow rate should be used according to temperature requirements.

Figure 9 shows transient response of the PVT system when mass flow is decreased from 0.002 kg/s to 0.001 kg/s. It does not take large amount of time to reach steady state. It requires 2-3 minutes to reach steady state.

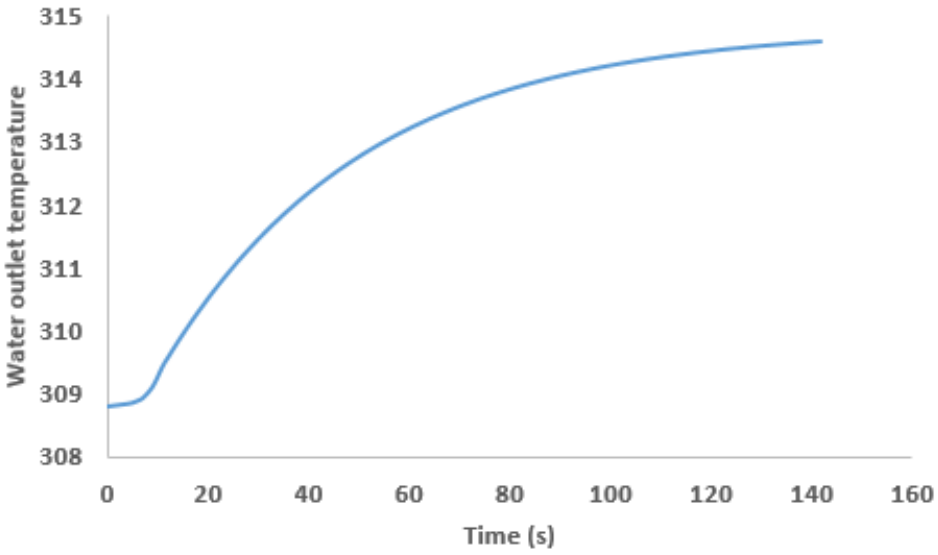

Figure 9: Transient response of PVT system

References

1. Chow, T. (2003). Performance analysis of photovoltaic-thermal collector by explicit dynamic model. *Solar Energy*, *75*(2), 143-152. https://doi.org/10.1016/j.solener.2003.07.00
2. Misha, S., Abdullah, A., Tamaldin, N., Rosli, M., & Sachit, F. (2020). Simulation CFD and experimental investigation of PVT water system under natural Malaysian weather conditions. *Energy Reports*, *6*, 28-44. https://doi.org/10.1016/j.egyr.2019.11.162
3. Wang, N., Zeng, S., Zhou, M., & Wang, S. (2015). Numerical study of flat plate solar collector with novel heat collecting components. *International Communications In Heat And Mass Transfer*, *69*, 18-22. https://doi.org/10.1016/j.icheatmasstransfer.2015.10.012
4. Selmi, M., Al-Khawaja, M., & Marafia, A. (2008). Validation of CFD simulation for flat plate solar energy collector. *Renewable Energy*, *33*(3), 383-387. https://doi.org/10.1016/j.renene.2007.02.003
5. Andrade Cando, A., Quitiaquez Sarzosa, W., & Toapanta, L. (2020). CFD Analysis of a solar flat plate collector with different cross sections. *Enfoque UTE*, *11*(2), 95-108. https://doi.org/10.29019/enfoque.v11n2.601
6. Fesharaki, V. J., Dehghani, M., Fesharaki, J. J., & Tavasoli, H. (2011, November). The effect of temperature on photovoltaic cell efficiency. In *Proceedings of the 1stInternational Conference on Emerging Trends in Energy Conservation–ETEC, Tehran, Iran* (pp. 20-21).